

Spatial distribution of potential soils to be sulfuric acids in coastal zones of Puerto Rico

Onix H. Cabezudo Vázquez

University of Puerto Rico at Mayaguez, Department of Agricultural Soil Science,

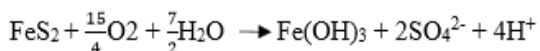
Email: onix.cabezudo@upr.edu

Abstract – Remote sensing is a valuable tool for determining acid sulphate soils is quite a challenge based on minerals in coastal zones. Based on the correlation of mineral and vegetation index using Sentinel 2A sensor there can be areas that can be unique to study in the field based on the wetlands selected. The wetlands are Caño Boqueron (Cabo Rojo), Jobo's Bay (Guayama), and Hiltons Wetland (Ponce), these areas have been identified as potential acid sulphate soils. The main objective is to identify potential areas to be sulfuric soils in the coastal areas of the wetlands selected. We used ENVI 5.3 and ArcMap 10.6 to conduct supervised classification, calculate vegetation and minerals index algorithms, and calculate statistics. Mineral index (Iron Oxide, Ferric Iron) and Vegetation index (NDVI) were correlated to establish potential areas that can be sample to determine potential areas. Caño Boqueron and Hilton Wetland gave an inversely proportional distribution given the Pearson correlation to the Fe 3+ index based on the NDVI.

Key words: acid sulphate soils, remote sensing, wetlands, index

Introduction

Acid sulphate soils remain largely "ecologically safe" while anoxic conditions prevail (Mosley, et al., 2017). However, exposure to air (physical disturbances or droughts) promotes sulphuration, a process by which soil minerals containing sulfides (pyrites) are oxidized, producing large amounts of sulfuric acid 'next reaction' (Beucher et al., 2016; Karimian et al., 2017; Payne and Stolt, 2017). The sulfurization process can create serious ecological damage in estuaries and coastal areas, causing large fish deaths and extreme degradation of concrete and steel structures (Fitzpatrick et al., 2017b).



The recognition of acid sulphate soils goes back to the 18th century, where they were referred to as "clay with sulfuric acid" (Pons, 1973). The terms "sulfidic materials" and "sulfuric horizon" were introduced in the United

States in the first formal classification system developed for these soils (Soil Taxonomy, 1975) (Fanning, et al., 2017). However, recognition and identification of CLASS is still an evolving science as the presence of these soils has gone largely undetected in many regions of the world where the deleterious impacts of the mismanagement of these soils is commonly attributed to other causes.

The Australian classification system, a country in which the presence of CLASS was not recognized until the 1990s, recognizes three main categories, namely: hyper-sulfidic soils, hypo-sulfide soils and mono-sulphide materials. (Fanning, et al., 2017). Mono-sulfide materials are those that undergo a color change, from black to gray, immediately after exposure to air, an indication of the presence of metastable iron sulphides (wetlands). The use of the pH results of the wet aerobic incubations is considered as the primary classification criterion of all the systems (Wessel, et al., 2017; Fanning, et al., 2017). On the other hand, hypo-sulfidic materials undergo

pH drop of 0.5 units or more during a 16-week moist aerobic incubation (MAI) to a final pH greater than 4.0. Finally, hyper-sulfidic materials also experience a pH drop greater than 0.5 units during MAI but reach a final pH lower than 4.0. The use of pH results from moist aerobic incubations is now regarded as the primary classification criteria by all systems (Wessel, et al., 2017; Fanning, et al., 2017). In Puerto Rico there's no soil classification for acid sulphate soils.

In this case study the cost side of Puerto Rico is being evaluated to identify this presence of acidity in the soils, basically the wetlands are study areas. Wetlands are areas where water covers the soil or is present on or near the soil surface throughout the year for varying periods during the year, including the growing season. Based on the USDS (2016) these areas are classified as Water soil, and are formed under conditions of saturation, flooding, or ponding for sufficient time in the growing season as allowing anaerobic conditions to occur in the upper part of the soil profile, in this case can be potential areas if they are pyrite in the soil profile. They can support both aquatic and terrestrial species. The presence of water creates conditions that favor the growth of specially adapted plants (hydrophytes) and promote the development of soils characteristic of wetlands (water) (EPA, 2012).

Rowan and John (2003) used the Advanced Spaceborne Thermal Emission and Reflection Radiometer (ASTER) sensor to evaluate images of the Mountain Pass, California areas indicating several lithologic groups using spectral-matching techniques. The three visible and six near-infrared bands, which have 15-m and 30-m resolution, respectively, were calibrated by using in situ measurements of spectral reflectance. Ferromuscovite, which is common in these intrusive rocks, was distinguished from Al-muscovite present in granitic gneisses and Mesozoic

granite. Bienworth et al. (2005) generates an application to identify sulfuric acid soil stains from radiometric gamma data of mineral spectrums that are proportionally inverse to acid sulphur and GIS analysis. And Bienworth et al. (2005) uses a similar method but with iron mineral spectrum and a hyperspectral sensor.

Scientific Question: Could the indicators help predict acid sulfuric soils given satellite images?

Objectives: General: Identify potential areas to be sulfuric soils in the coastal areas of Jobos Bay, Caño Boquerón and Ponce Hilton. Specific: Use vegetation and mineral indices to identify potential areas to be sampled with multi-spectral sensor.

Material and Methods

A. Images

The image selected to analyze the potential acid sulfate soils corresponded to Sentinel 2A, of December 9, 2018. This is a 12 bands multispectral sensor with spectral information between the visible and mid infrared spectrum. It has 10 m spatial resolution in the visible spectrum and 1 band in the near infrared spectrum, 20 m spatial resolution in some Vegetation Red Edges (red to infrared spectrum) and SWIR, and 60 m spatial resolution the SWIR and Coastal aerosol bands. The image was retrieved from the Earth Explorer (2000) database, based on minimum clouds.

Sentinel-2 Bands	Central Wavelength (µm)	Resolution (m)
Band 1 - Coastal aerosol	0.443	60
Band 2 - Blue	0.490	10
Band 3 - Green	0.560	10
Band 4 - Red	0.665	10
Band 5 - Vegetation Red Edge	0.705	20
Band 6 - Vegetation Red Edge	0.740	20
Band 7 - Vegetation Red Edge	0.783	20
Band 8 - NIR	0.842	10
Band 8A - Vegetation Red Edge	0.865	20
Band 9 - Water vapour	0.945	60
Band 10 - SWIR - Cirrus	1.375	60
Band 11 - SWIR	1.610	20
Band 12 - SWIR	2.190	20

Image 1. Sentinel 2A sensor description

B. Acid Sulphate Soils indicators

Based on visual and chemical interpretations we can determine acid sulphate soils (Beucher et al., 2016, Fitzpatrick et al., 2017, Wessel, et al., 2017; Fanning, et al., 2017). Some of the indicators are aerobic incubated pH (< 5), minerals (pyrite, iron oxide, jarosite, swerminate, ferric iron etc.), oil films in the superficial water (bacterias), and death of vegetation of moribund state.

C. Sentinel 2A index applied

i. NDVI

The normalized difference vegetation index (NDVI), which is derived from remote-sensing (satellite) data, is closely linked to drought conditions. To determine the density of green on a patch of land, the distinct colors (wavelengths) of visible and near-infrared sunlight reflected by the plants are observed. Range of NDVI is -1 to +1. Higher value of NDVI refers to healthy and dense vegetation and lower NDVI values show sparse vegetation:

$$NDVI = \frac{NIR - RED}{NIR + RED}$$

Where: NIR = band 5 ; RED = band 4

where RED and NIR stand for the spectral reflectance measurements acquired in the red (visible) and near-infrared regions, respectively (Drisy et al., 2018).

ii. Iron Oxide and Iron Ferric (Fe²⁺ and Fe³⁺) Index

Based on the results of Rowan and John (2003) from Aster and some comparisons between this sensor and the Sentinel 2A, Henrich (2009) created an online index databased related to the Sentinel 2A sensor and the iron derivate index where created and used in this study. Where some of the algorithms are based on the visible spectrum and near and mid infrared.

$$\text{Iron oxide} = \frac{\text{band 11}}{\text{band 8}}$$

$$Fe^{2+} = \left(\frac{\text{band 12}}{\text{band 8}} \right) + \left(\frac{\text{band 3}}{\text{band 4}} \right)$$

$$Fe^{3+} = \frac{\text{band 4}}{\text{band 8}}$$

Based on the indicators to determine potential acid sulphate soils like the mineral precipitated in the soil surface this index for this sensor where selected.

D. Description of study area

The areas selected for this case of study are based on potential acid sulphate soils that have been classified with previous soil samples recollected in those areas (Image 2). They are in the western and southern coastal areas of Puerto Rico: Caño Boqueron at the wester side coast, Ponce Hilton Wetland and Jobo's Bay at the southern side coast of Puerto Rico. Caño Boqueron Wetland is at the Boqueron Bay where the Boqueron Wildlife Refuge is located and its managed by the Department of Natural and Environmental Resources. The Caño consist of the protected area and the wetland areas, it's has an area approximated 5 km². The Jobos Bay National Research Reserve is the second largest estuarine area of Puerto Rico. It expands between the towns of Guayama and Salinas (aprox. 14 km²) and its grounds were acquired by the Department of Natural and Environmental Resources in 1981 and was designated as Jobos Bay National Estuarine Research Reserve by the National Oceanic and Atmospheric Administration (NOAA) as part of the National Estuarine Research Reserve System (NERRS) (DRNA, 2019). The final areas selected to study is a wetland next to the Hilton Casino and Restaurant Resort in Ponce, this area isn't regulated by any federal agency like the DRNA and the approximated area of this wetlands is 11 km². The classification of this types of wetlands based on the Fish and Wildlife are Estuarine and Marine Deep-Water Wetlands for the wetlands selected (USGS, 2015), due to the intrusion of saline water of the beach.

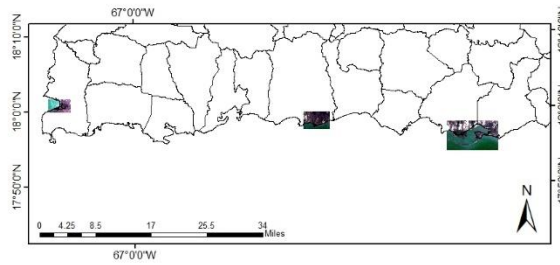


Image 2. Spatial distribution of the Jobo's Bay, Caño Boqueron, and Ponce Wetlands in the coast side of Puerto Rico

E. Image Processing

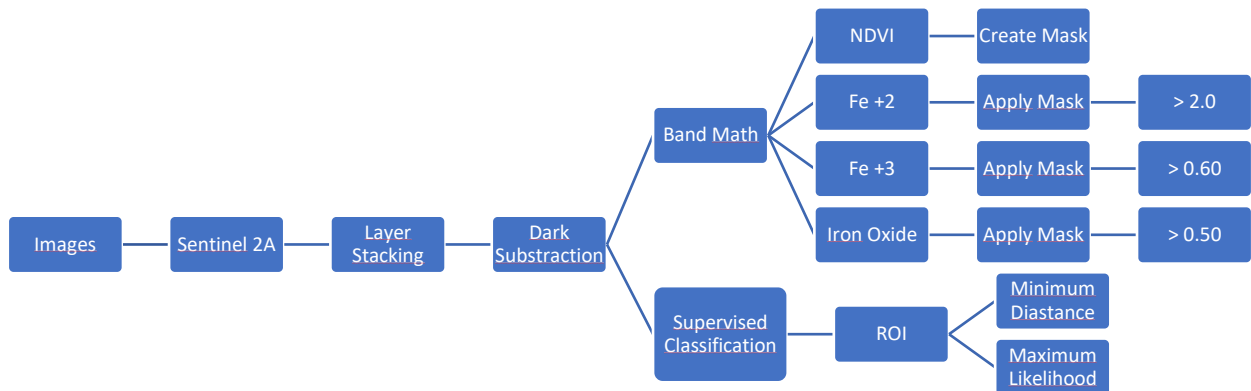


Image 3. Flow chart based on the process generated in ENVI and ArcMap 10.6 program

Based on the image retrieve from Earth Explorer different steps in ENVI and ArcMap 10.6 where conducted to analyses was made (Image 3).

In the interpretation in the image 3, we used layer stacking to combine the band necessary to estimate the index selected and a dark subtraction to clean the atmospheric reflection. Then based on empirical knowledge we trained potential areas due to the precipitated iron (reddish or dark orange color) and used a minimum distance and maximum likelihood supervised classification. Then, due the dark subtraction we used band math to apply all the

algorithms of each index, then based on the NDVI a mask was created and applied to all the mineral and vegetation index. Those results where exported to ArcMap 10.6 to create areas of interest based on high values of mineral index and determine if those values correlate with the values of the NDVI. The data was create using Create Random Points in the polygons of each index, and an Extract Multi Value to Points of each Index and the NDVI values. This data was exported to Excel and applied a Pearson Correlation to determine if there's a distribution to the data.

Results and Discussion

A. Hilton's Casino and Golf Resort Wetland, Ponce

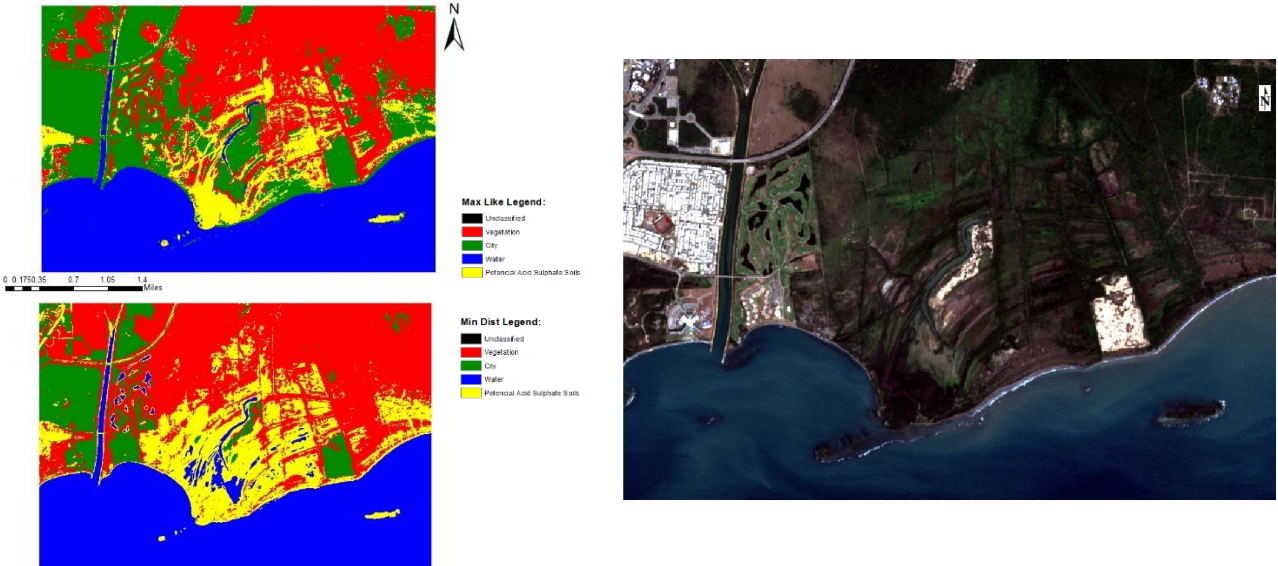


Image 4. Maximum Likelihood and Minimum Distance supervised classification for the Wetland next to Ponce Hilton Resort.

For this image 4, yellow of this classification represents the Potential Acid Sulfate Soils. Due to the RGB image of this area and the trained area, the Maximum Likelihood Classification is more suited to the areas that can have precipitated iron based on the color of the surface in the soil. The city, water, and vegetated classification are more well distribute in the Maximum Likelihood Classification.

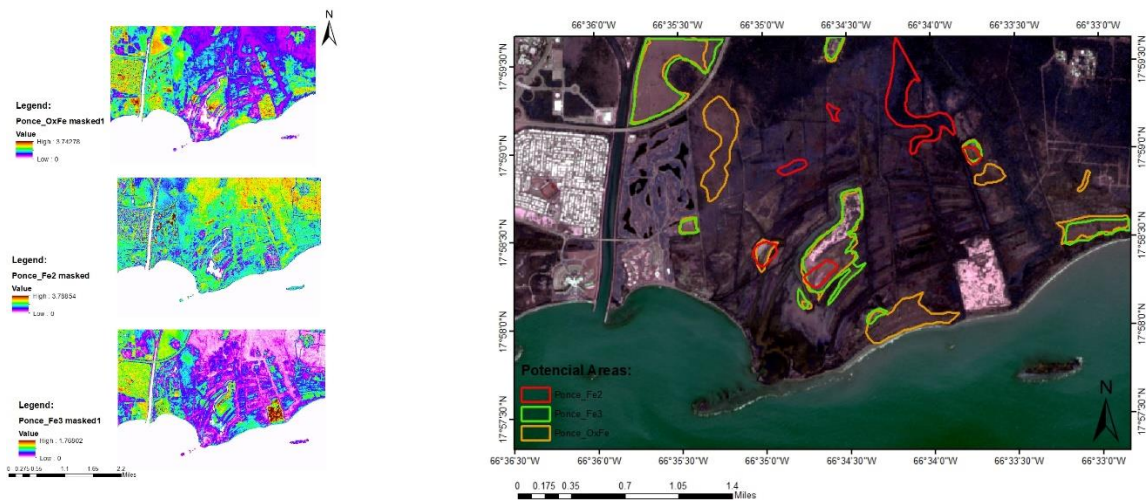


Image 5. Iron Oxide and Iron Ferric Index applied for the Wetland next to Ponce Hilton Resort

The image 5 the mineral index is represented at the Ponce Hilton Resort Wetland, and the maximum of each mineral index was converted into polygon and represented in the RGB satellite image of the zone. Iron Oxide and Fe 3+ data intersect in some areas more in comparison with Fe 2+ data, some bare soils areas are detected by the polygons of the Oxide and Fe 3+ and that can be an indicator that in those areas are more precipitated iron. And based on image 6 we can see that on the NDVI zones with lower value the Iron Oxide and Fe 3+ have higher values. Based on Person's correlation comparing the NDVI and the minerals (Annex, Graph 1 – 3), Fe 3+ has -0.72 (inversely proportional), Iron Oxide has -0.62 (inversely proportional), and Fe 2+ has 0.31 (directly proportional), but in consideration for the samples the one the Fe3+ index is more suitable. Indicating that in areas where there is minimum vegetation biomass based on the NDVI there can be more precipitated Fe3+ iron in the soil.

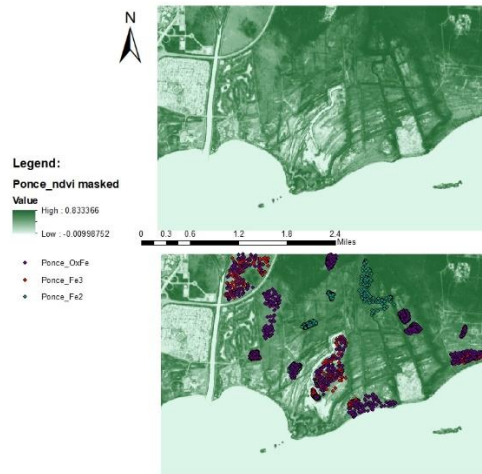


Image 6. NDVI index at Ponce Hilton Wetland and the values of the mineral index

B. Jobos Bay Wetland, Guayama

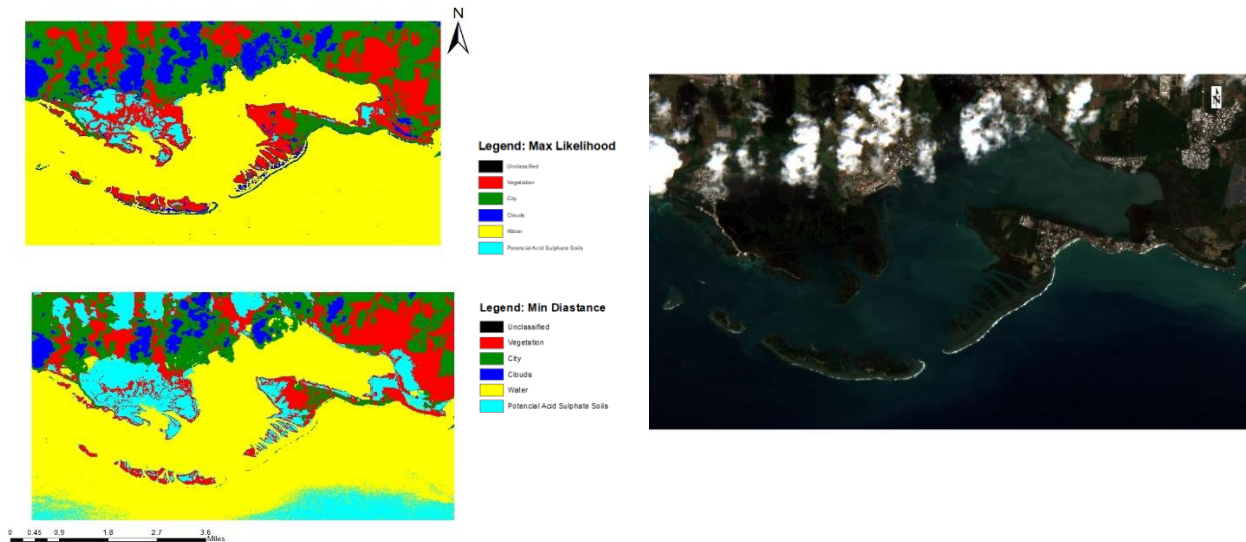


Image 7. Maximum Likelihood and Minimum Distance supervised classification for the Jobo's Bay Wetland

For this image 7, blue of this classification represents the Potential Acid Sulfate Soils. Due to the RGB image of this area and the trained area, the Maximum Likelihood Classification is more suited to the areas that can have precipitated iron based on the color of the surface in the soil. The water, and vegetated classification are more well distribute in the Maximum Likelihood Classification. Bur based on the image there are clouds interfering in some costal areas.

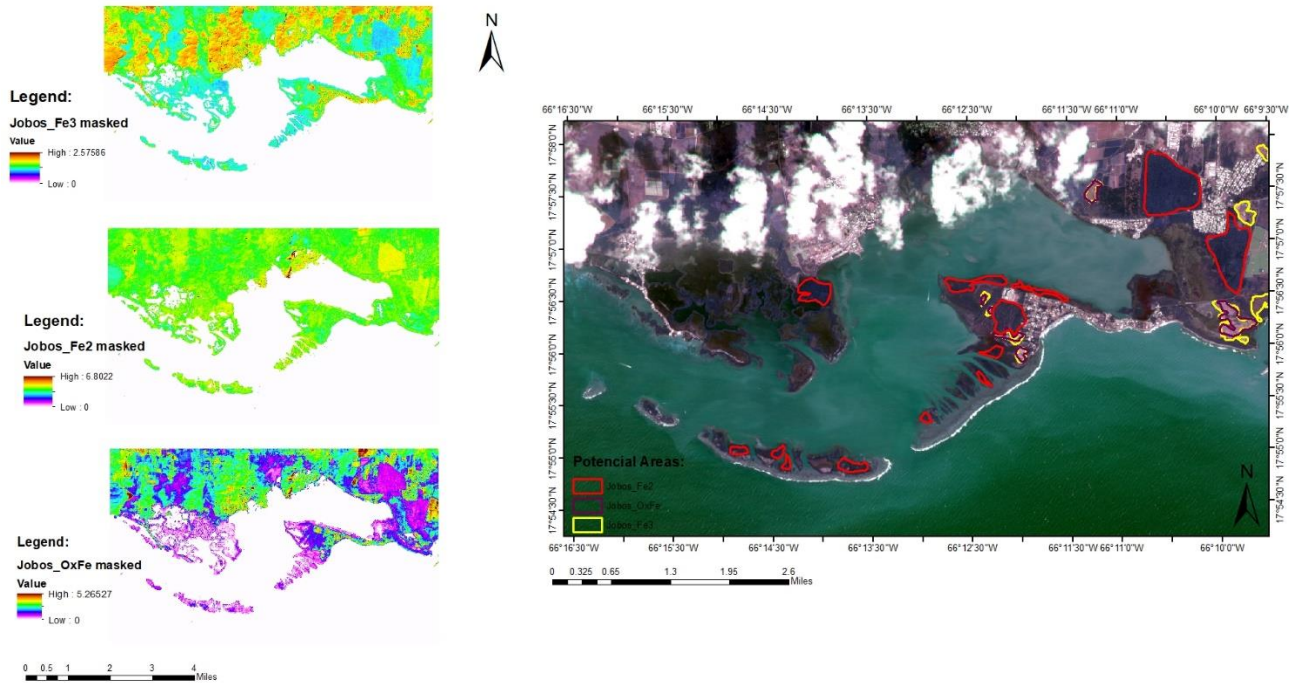


Image 8. Iron Oxide and Iron Ferric Index applied for the Jobo's Bay Wetland

The image 8 the mineral index is represented at the Jobo's Bay Wetland, and the maximum of each mineral index was converted into polygon and represented in the RGB satellite image of the zone. Iron Oxide and Fe 3+ data intersect in some areas more in comparison with Fe 2+ data, the bare soils areas are detected by the polygons of the Oxide and Fe 3+ and that can be an indicator that in those areas are more precipitated iron and on the contrary areas with more NDVI has more higher values on the Fe 2+ index. Based on image 9 we can see that on the NDVI zones with lower value the Iron Oxide and Fe 3+ have higher values, and NDVI zones with higher values to the Fe2+ index. Based on Person's correlation comparing the NDVI and the minerals (Annex, Graph 4 – 6), Fe 3+ has -0.49 (inversely proportional), Iron Oxide has -0.52 (inversely proportional), and Fe 2+ has 0.69 (directly proportional), but in consideration for the samples the one the Fe 2+ index is more suitable. Indicating that in areas where there is more vegetation biomass based on the NDVI there can be more precipitated Fe2+ iron in the vegetation, possible due to the micronutrients that the plant's needs.

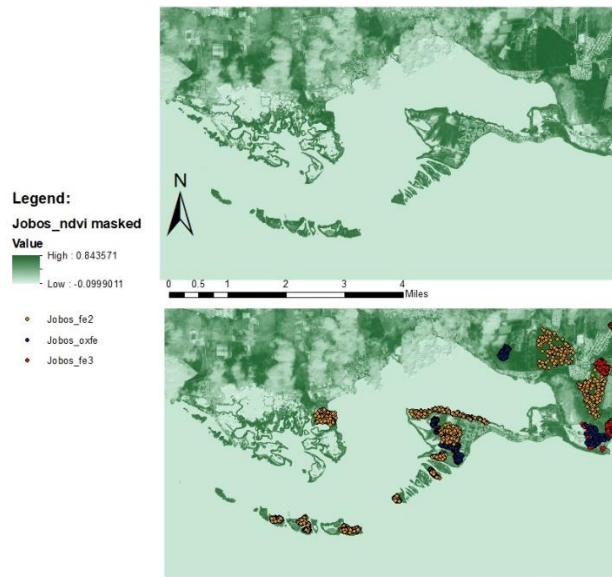


Image 9. NDVI index at Jobo's Bay Wetland and the values of the mineral index

C. Caño Boqueron Wetland, Cabo Rojo

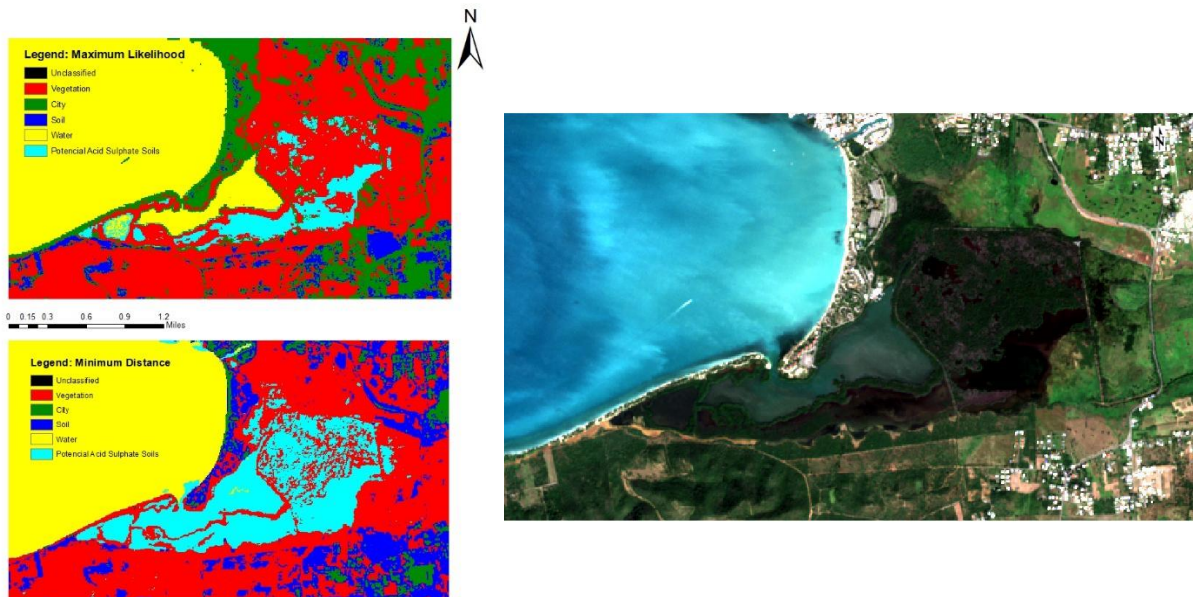


Image 10. Maximum Likelihood and Minimum Distance supervised classification for the Caño Boqueron Wetland at Cabo Rojo

For this image 10, blue of this classification represents the Potential Acid Sulfate Soils. Due to the RGB image of this area and the trained area, the Maximum Likelihood Classification is more suited to the areas that can have precipitated iron based on the color of the surface in the soil. The city, water, and vegetated classification are more well distribute in the Maximum Likelihood Classification.

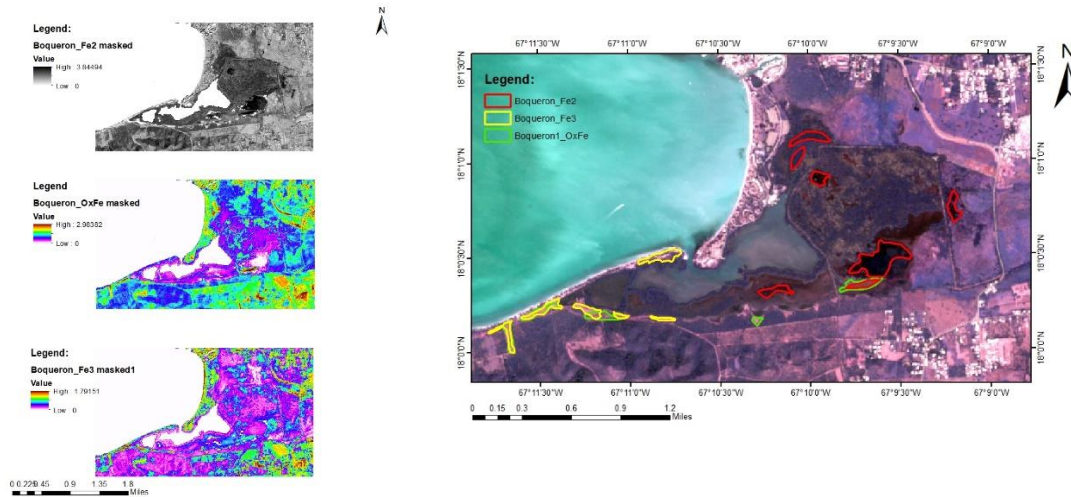


Image 11. Iron Oxide and Iron Ferric Index applied for the Caño Boqueron Wetland at Cabo Rojo

The image 11 the mineral index is represented at the Jobo's Bay Wetland, and the maximum of each mineral index was converted into polygon and represented in the RGB satellite image of the zone. Iron Oxide and Fe 3+ data intersect in some areas more in comparison with Fe 2+ data, some bare soils areas are detected by the polygons of the Oxide and Fe 3+ and that can be an indicator that in those areas are more precipitated iron.

On image 12 we can see that on the NDVI zones with lower value the Iron Oxide and Fe 3+ have higher values, and NDVI zones with higher values to the Fe2+ index. Based on Person's correlation comparing the NDVI and the minerals (Annex, Graph 7 – 9), Fe 3+ has -0.76 (inversely proportional), Iron Oxide has -0.68 (inversely proportional), and Fe 2+ has -0.16 (inversely proportional), but in consideration for the samples the one the Fe 3+ index is more suitable. Indicating that in areas where there is minimum vegetation biomass based on the NDVI there can be more precipitated Fe3+ iron in the soil.

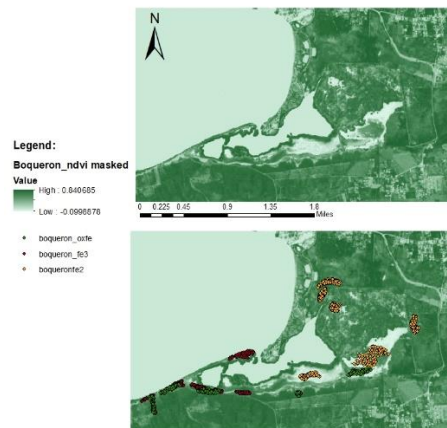


Image 12. NDVI index at Caño Boqueron Wetland at Cabo Rojo and the values of the mineral index

D. Overall results

In the table 1 gives the statistics representation of each Person correlation based on the minerals index and the vegetation index. Based on the results the best areas to infer potential areas to sample is the Fe³⁺ due to the Caño Boqueron (-0.76) and Ponces (-0.72) correlation index results. In Jobo's Bay results the Fe²⁺ gave a high correlation but the graph 6 at the annex, the relationship between the mineral index and the NDVI was that the more the vegetation biomass the more the Fe²⁺ index is, and based in the indicators to determine potential acid sulphate soils we need degradation on the vegetation.

Table 1. Pearson correlation given each mineral index with respect to the vegetation index (NDVI), in each place of interest.

AREAS	MINERAL	PEARSON	R ²
Boqueron	OxFe	-0.67993	0.46
Boquerón	Fe3	-0.75731	0.57
Boqueron	Fe2	-0.15736	0.03
Jobos	OxFe	-0.52468	0.28
Jobos	Fe3	-0.49229	0.24
Jobos	Fe2	0.689965	0.48
Ponce	OxFe	-0.62128	0.39
Ponce	Fe3	-0.71989	0.51
Ponce	Fe2	0.305353	0.09

Limitations and Recommendations

Not having created a mask for the cloudiness and city, could have generated alterations to the values of each applied index. Where the supervised classifications were going to be applied and to be able to establish the areas of greatest impact of each index with more precision. For this model, other variables can help describe these areas of interest like soil moisture and the water table for the prediction. A comparison based on time it would give a good distribution of the index applied, and the correlations of the minerals with respect to the NDVI were different with respect to the data obtained now (exam.: dry season vs wet season), due to the hydrological change that predominates in the coastal areas. The mineral index would be more credible based on field validation to determine if there are those types

of minerals exist based on the data of the mineral index. Spectral data of the mineral derived from pyrite can be another classification but due to the humidity and vegetation would be difficult to identify the minerals.

Conclusion

The supervised classification given the indicator of the color of the precipitated iron (dark red or orange) could help us to identify or infer potential areas to be sulphic acid soils, but it had its limitations. The classifications supervised with empirical criteria (color) for this identification method can help determine areas with the characteristics that are being sought.

We can associate areas to collect soil samples given the Fe³⁺ index and Iron Oxide, since these showed an inversely proportional correlation given the Pearson correlation. Where the areas with the highest mineral index would be chosen

to collect soil samples such as: Caño Boquerón and Ponce.

Literature Cited

- Beucher, A., K. Adhikari, H. Breuning-Madsen, M.B. Greve, P. Österholm, S. Fröjdö, N.H. Jensen, and M.H. Greve. 2016. Mapping potential acid sulfate soils in Denmark using legacy data and LiDAR-based derivatives. <http://dx.doi.org/10.1016/j.geoderma.2016.06.001>
- Departamento de Recursos Naturales. (2019). JBNERR. Retrieved from <http://drna.pr.gov/jbnerr/>
- Drisy, J., D. S. K., & Roshni, T. (2018). Spatiotemporal Variability of Soil Moisture and Drought Estimation Using a Distributed Hydrological Model. *Integrating Disaster Science and Management*, 451–460. doi:10.1016/b978-0-12-812056-9.00027-0
- Earth Explorer; 2000; FS; 083-00; Geological Survey (U.S.), <https://earthexplorer.usgs.gov/>
- Environmental Protection Agency 2012. What are Wetlands. <http://water.epa.gov/type/wetlands/wh at.cfm>
- Fanning, D.S., M.C. Rabenhorst, and R.W. Fitzpatrick. 2017. Historical developments in the understanding of acid sulfate soils. *Geoderma*. 308: 191-206.
- Fitzpatrick, R.W., P. Shand, and L.M. Mosley. 2017b. Acid sulfate soil evolution models and pedogenic pathways during drought and reflooding cycles in irrigated areas and adjacent natural wetlands. *Geoderma*. 308: 270-290.
- Hasmadi, M., Akmar, C.K., C.K.O., Norsaliza, U. and Kasawani, I. 2010. Comparison of several vegetation indices for mangrove mapping using remotely sensed data. *International Geoinformatics Research and Development Journal*. Vol. 1, Issue 3.
- Henrich, V., Jung, A., Götze, C., Sandow, C., Thürkow, D., Gläßer, C. (2009): **Development of an online indices database: Motivation, concept and implementation.** 6th EARSeL Imaging Spectroscopy SIG Workshop Innovative Tool for Scientific and Commercial Environment Applications Tel Aviv, Israel, March 16-18, 2009. ([PDF](#))
- Karimian, N. S.G. Johnston, and E.D. Burton. 2017. Acidity generation accompanying iron and sulfur transformations during drought simulations of freshwater re-flooded acid sulfate soils. *Geoderma*. 285: 117-131.
- Mosley, L.M., T.K. Biswas, F.J. Cook, P. Marschner, D. Palmer, P. Shand, C. Yuan, R.W. Fitzpatrick. 2017. Prolonged recovery of acid sulfate soils with sulfuric materials following severe drought: causes and implications. *Geoderma*. 38: 312-320.
- NASA. (2019). Sentinel-2A Launches—Our Compliments & Our Complements. Retrieved from <https://landsat.gsfc.nasa.gov/sentinel-2a-launches-our-compliments-our-complements/>
- Payne, M.K. and M.H. Stolt. 2017. Understanding sulfide distribution in subaqueous soil systems in southern England, USA. *Geoderma*. 308: 207-214.

Pons, L.J. 1973. Outline of the genesis, characteristics, cICLASSification and improvement of acid sulfate soils. In Dost, H. (Ed.), Proceedings of the 1972 (Wageningen, Netherlands) Int. Acid Sulfate Soils Symposium. Int. Land Reclamation Inst. Publication 18, Wageningen, The Netherlands, Vol. 1, 3-27.

Rowan, L. C., & Mars, J. C. (2003). Lithologic mapping in the Mountain Pass, California area using Advanced Spaceborne Thermal Emission and Reflection Radiometer (ASTER) data. Remote Sensing of Environment, 84(3), 350–366.
doi:10.1016/s0034-4257(02)00127-x

U. S. Fish and Wildlife Service. Publication date (2015). National Wetlands Inventory

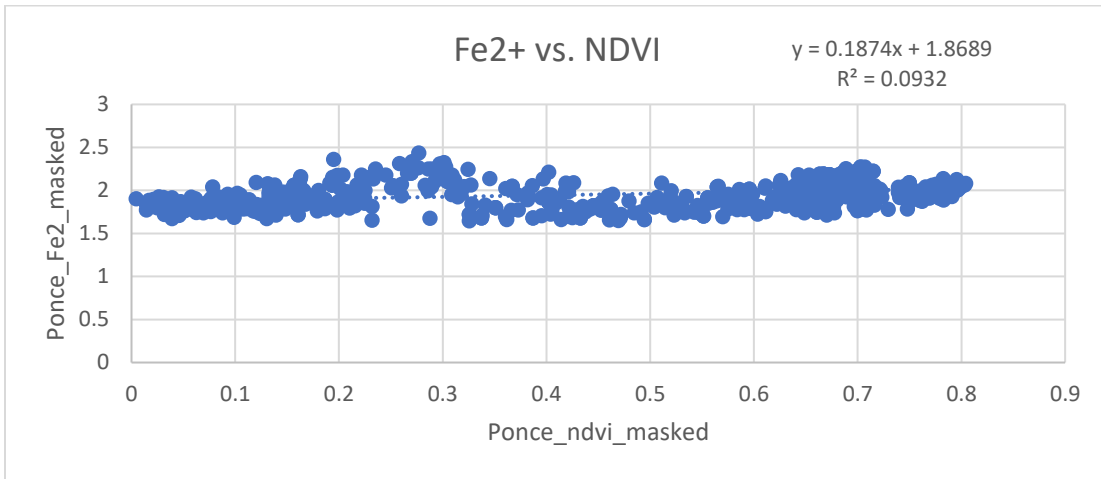
website. U.S. Department of the Interior, Fish and Wildlife Service, Washington, D.C.
<http://www.fws.gov/wetlands/>

USDA. (2016). Suelos hídricos según la USDA (Departamento de Agricultura de EE.UU.). Retrieved from
<https://www.madrimasd.org/blogs/universo/2016/04/25/147092>

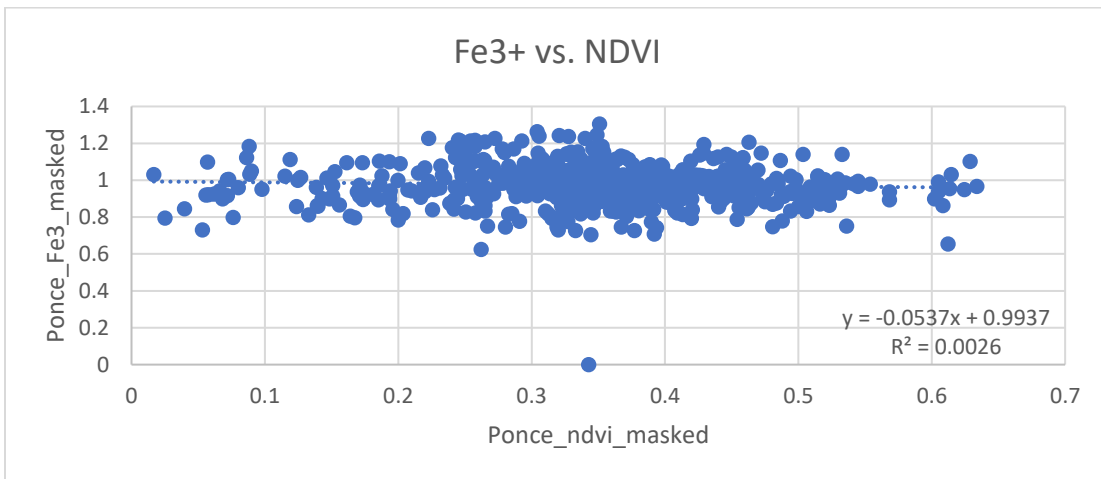
Wessel, B.M., M.C. Rabenhorst. 2017. Identification of sulfidic materials in the Rhode River subestuary of Chesapeake Bay. Geoderma. 308: 215-225

Wessel, B.M., M.C. Rabenhorst. 2017. Identification of sulfidic materials in the Rhode River subestuary of Chesapeake Bay. Geoderma. 308: 215-225.

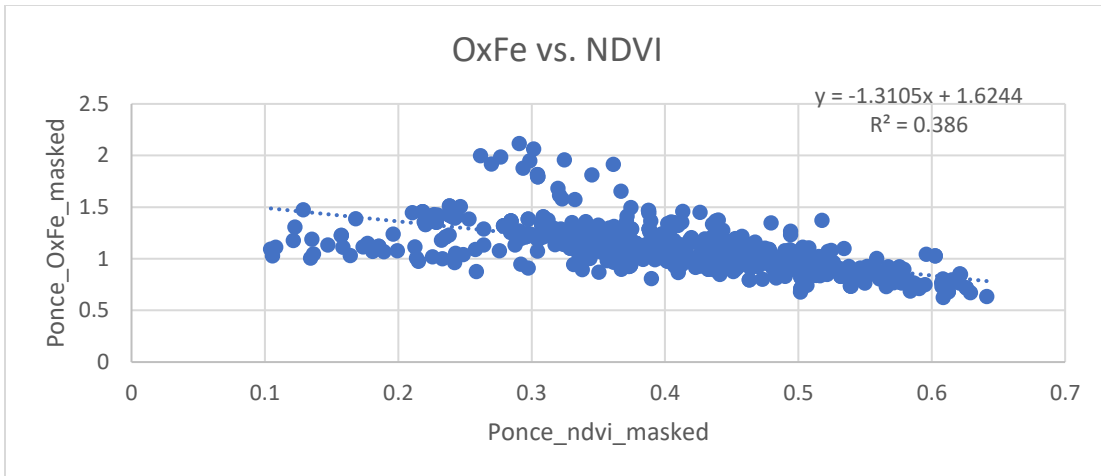
Appendix



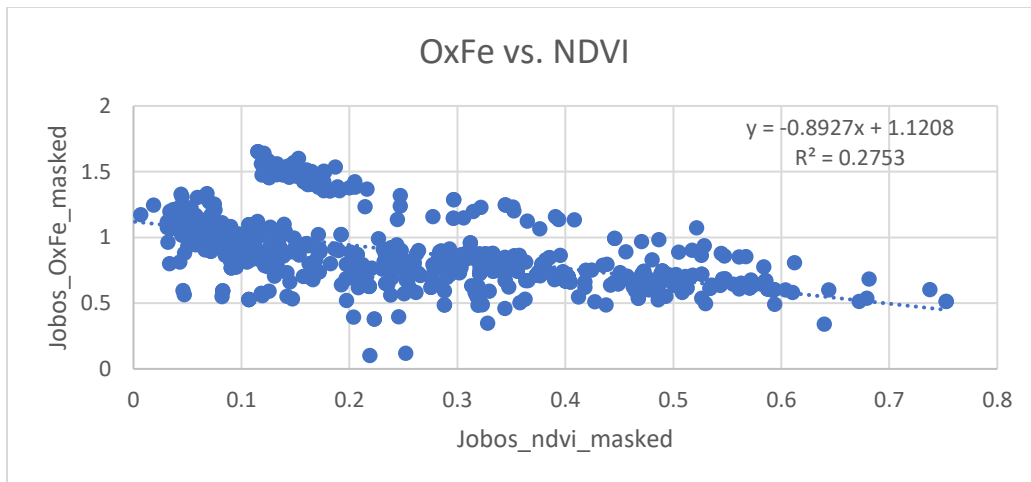
Graph 1. Pearson's correlation based on the Fe2+ mineral index and NDVI index on Ponce Hiltons Resort Wetland



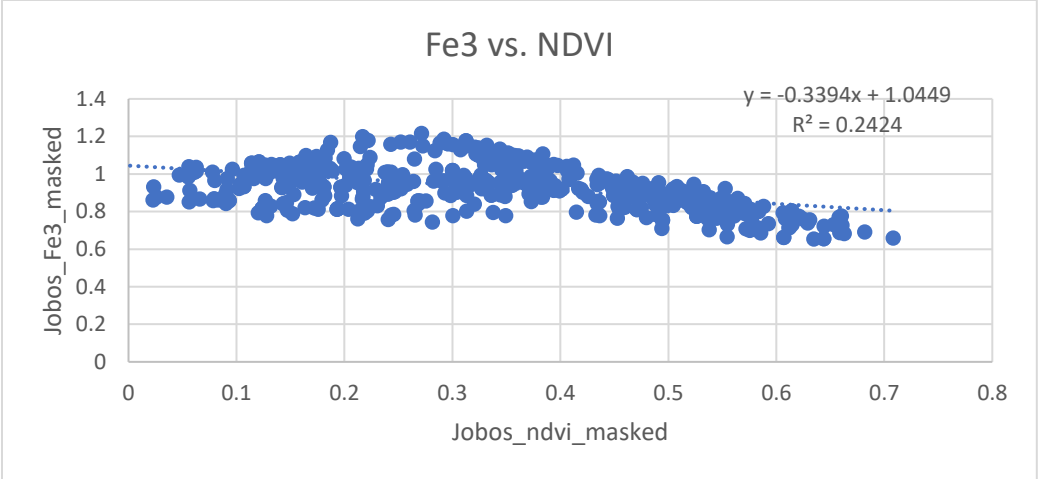
Graph 2. Pearson's correlation based on the Fe3+ mineral index and NDVI index on Ponce Hiltons Resort Wetland



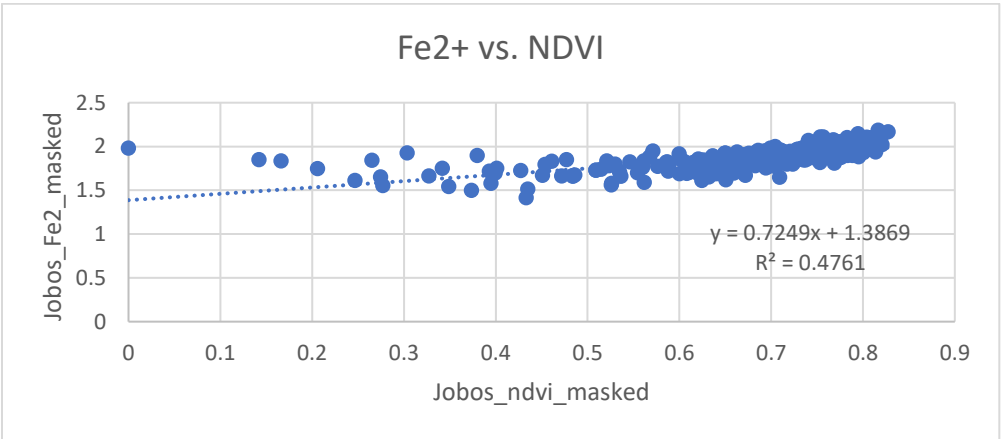
Graph 3. Pearson's correlation based on the Iron Oxide mineral index and NDVI index on Ponce Hiltons Resort Wetland



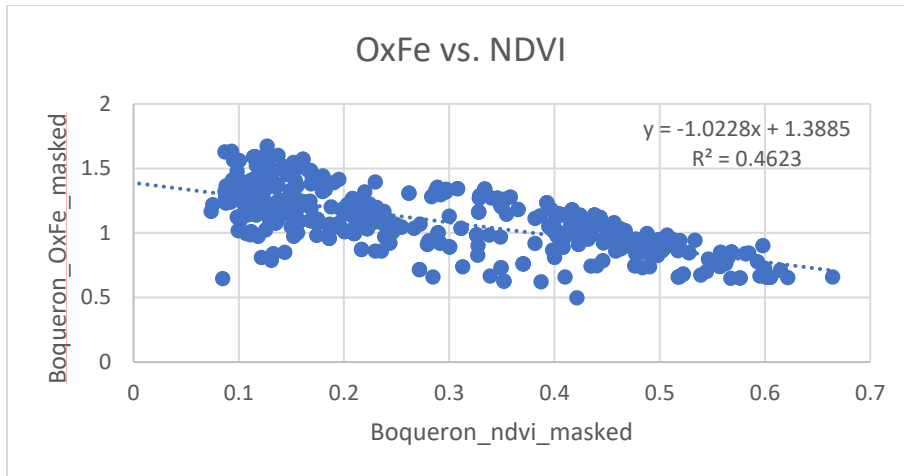
Graph 4. Pearson's correlation based on the Iron Oxide mineral index and NDVI index on Jobo's Bay Wetland



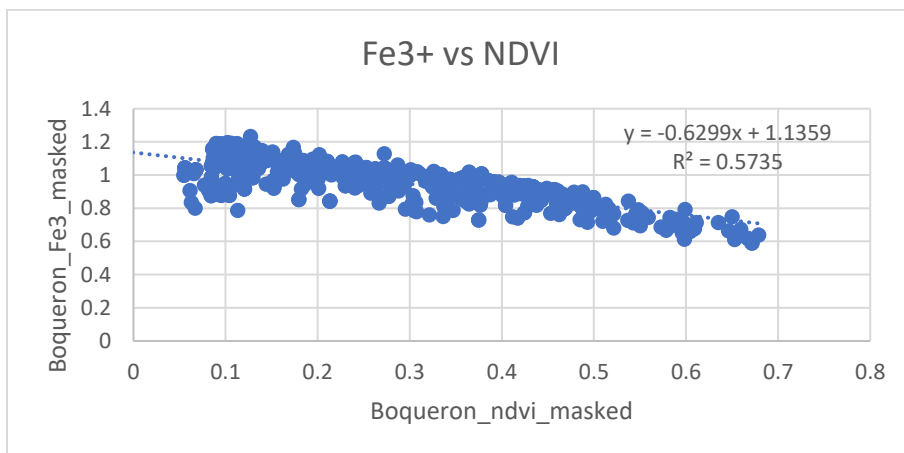
Graph 5. Pearson’s correlation based on the Fe3+ mineral index and NDVI index on Jobo’s Bay Wetland



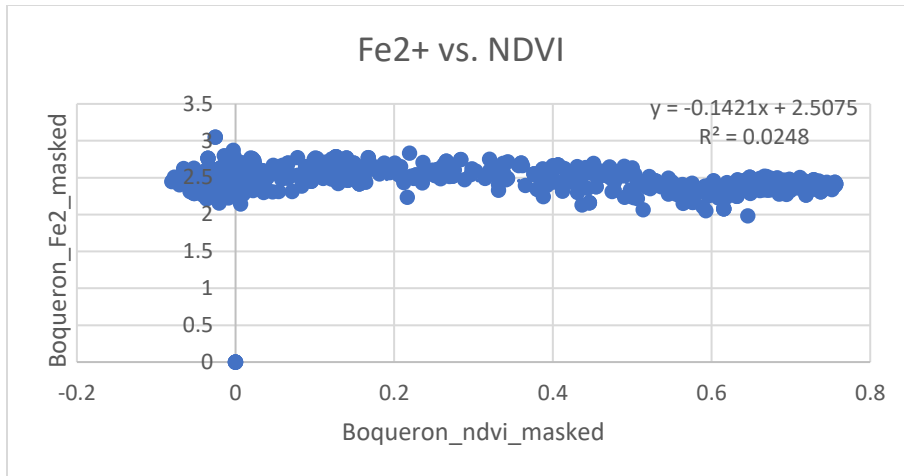
Graph 6. Pearson’s correlation based on the Fe2+ mineral index and NDVI index on Jobo’s Bay Wetland



Graph 7. Pearson's correlation based on the Iron Oxide mineral index and NDVI index on Caño Boqueron at Cabo Rojo



Graph 8. Pearson's correlation based on the Fe3+ mineral index and NDVI index on Caño Boqueron at Cabo Rojo



Graph 9. Pearson's correlation based on the Fe2+ mineral index and NDVI index on Caño Boqueron at Cabo Rojo